JVI Journals.ASM.org

Inhibition of Histone Deacetylase Activity Aggravates Coxsackievirus B3-Induced Myocarditis by Promoting Viral Replication and Myocardial Apoptosis

Lei Zhou,[a] Xiran He,[a] Bo Gao,[a] Sidong Xiong[a,b]

Institute for Immunobiology, Department of Immunology, Shanghai Medical College of Fudan University, Shanghai, China[a]; Jiangsu Key Laboratory of Infection and Immunity, Institutes of Biology and Medical Sciences, Soochow University, Suzhou, China[b]

ABSTRACT

Viral myocarditis, which is most prevalently caused by coxsackievirus B3 (CVB3), is a serious clinical condition characterized by excessive myocardial inflammation. Recent studies suggest that regulation of protein acetylation levels by inhibiting histone deacetylase (HDAC) activity modulates inflammatory response and shows promise as a therapy for several inflammatory diseases. However, the role of HDAC activity in viral myocarditis is still not fully understood. Here, we aim to investigate the role of HDAC activity in viral myocarditis and its underlying mechanism. CVB3-infected BALB/c mice were treated with the HDAC inhibitor (HDACI) suberoylanilide hydroxamic acid (SAHA) or trichostatin A (TSA). We found inhibition of HDAC activity aggravated rather than ameliorated the severity of CVB3-induced myocarditis, which was contrary to our expectations. The aggravated myocarditis by HDACI treatment seemed not to be caused by an elevated inflammatory response but by the increased CVB3 replication. Further, it was revealed that the increased CVB3 replication was closely associated with the HDACI-enhanced autophagosome formation. Inhibition of autophagosome formation by wortmannin or ATG5 short hairpin RNA dramatically suppressed the HDACI-increased CVB3 replication. The increased viral replication subsequently elevated CVB3-induced myocardial apoptosis. Conversely, inhibition of CVB3 replication and ensuing myocardial apoptosis by the antiviral drug ribavirin significantly reversed the HDACI-aggravated viral myocarditis. In conclusion, we elucidate that the inhibition of HDAC activity increases CVB3 replication and ensuing myocardial apoptosis, resulting in aggravated viral myocarditis. Possible adverse consequences of administering HDACI should be considered in patients infected (or coinfected) with CVB3.

IMPORTANCE

Viral myocarditis, which is most prevalently caused by CVB3, is characterized by excessive myocardial inflammation. Inhibition of HDAC activity was originally identified as a powerful anti-cancer therapeutic strategy and was recently found to be implicated in the regulation of inflammatory response. HDACI has been demonstrated to be efficacious in animal models of several inflammatory diseases. Thus, we hypothesize that inhibition of HDAC activity also protects against CVB3-induced viral myocarditis. Surprisingly, we found inhibition of HDAC activity enhanced myocardial autophagosome formation, which led to the elevated CVB3 viral replication and ensuing increased myocardial apoptosis. Viral myocarditis was eventually aggravated rather than ameliorated by HDAC inhibition. In conclusion, we elucidate the role of HDAC activity in viral myocarditis. Moreover, given the importance of HDACI in preclinical and clinical treatments, the possible unfavorable effect of HDACI should be carefully evaluated in patients infected with viruses, including CVB3.

Coxsackievirus B3 (CVB3) is a single-stranded positive-sense RNA virus of the genus *Enterovirus* in the *Picornaviridae* family (1). CVB3 is considered the most commonly identified infectious agent that causes viral myocarditis and has been linked to the ensuing development of dilated cardiomyopathy (DCM) (2). CVB3-induced cardiac injury is caused either by a direct cytopathic effect (CPE) of the virus or through inflammation-mediated mechanisms (3–6).

Many clinical studies have revealed that tumor necrosis factor-α (TNF-α), interleukin-6 (IL-6), and other proinflammatory cytokines play a crucial role in the pathogenesis of cardiac injury in myocarditis (7, 8). Therefore, modulation of inflammatory response is considered a potential therapeutic strategy for viral myocarditis. In fact, we have previously demonstrated that the shift of Th1 to Th2 inflammatory responses could alleviate the myocarditis severity (9–11). We also found that A20 (also known as tumor necrosis factor alpha-induced protein 3, or TNFAIP3) protected against CVB3-induced myocarditis by inhibiting inflammatory response (12). More recently, we demonstrated an essential role of pyrin domain containing 3

Received 22 April 2015 **Accepted** 28 July 2015

Accepted manuscript posted online 12 August 2015

Citation Zhou L, He X, Gao B, Xiong S. 2015. Inhibition of histone deacetylase activity aggravates coxsackievirus B3-induced myocarditis by promoting viral replication and myocardial apoptosis. J Virol 89:10512–10523. doi:10.1128/JVI.01028-15.

Editor: K. Kirkegaard

Address correspondence to Bo Gao, gaobo@fudan.edu.cn, or Sidong Xiong, sdxiongfd@126.com.

doi:10.1128/JVI.01028-15

(NLRP3) activation and IL-1β secretion in mediating the pathological response to CVB3 infection (13).

As a major form of epigenetic mechanism, acetylation modification of both histone and nonhistone proteins is governed by the opposing activities of histone acetyltransferases (HAT) and histone deacetylases (HDAC). HDAC plays a key role in the homeostasis of the acetylation level (14). Inhibition of HDAC activity was originally identified as a powerful anti-cancer therapeutic strategy and was recently found to be implicated in the regulation of the inflammatory response (15). We have previously reported the important effect of HDAC activity on IFN-stimulated gene induction (16). Of note, HDAC inhibitor (HDACI) has been demonstrated to be efficacious in animal models of several inflammatory diseases, such as arthritis (17), colitis (18), graft versus host disease (19), systemic lupus erythematosus (SLE) (20), and septic shock (21). Thus, it is reasonable to hypothesize that HDACI plays a protective role in viral myocarditis. To this end, in the present study, we explored the role of HDAC activity in CVB3-induced viral myocarditis.

Our results suggested that inhibition of HDAC activity by HDACI suppressed proinflammatory cytokine expression, as expected. However, we found that HDACI enhanced myocardial autophagosome formation, which led to the elevated CVB3 viral replication and ensuing increased myocardial apoptosis. Consequently, viral myocarditis was aggravated rather than ameliorated by HDACI treatment. We elucidate the role of HDAC activity in the pathogenesis of viral myocarditis. Possible side effects of clinically administering HDACI should be fully considered in patients infected with viruses, including CVB3.

MATERIALS AND METHODS

Cell culture, mice, and virus. HeLa cells were grown and maintained in Dulbecco's modified Eagle's medium (DMEM) supplemented with 10% heat-inactivated fetal bovine serum. Five-week-old male BALB/c mice were purchased from the Department of Laboratory Animal Science of Fudan University. All animal experiments were performed according to the Guide for the Care and Use of Medical Laboratory Animals (Ministry of Health, People's Republic of China, 1998) and with the ethical approval of the Shanghai Medical Laboratory Animal Care and Use Committee (permit number SYXK 2009-0036), as well as the Ethical Committee of Fudan University (permit number 2009016). CVB3 (Nancy strain) was propagated in HeLa cells (ATCC CCL-2) and stored at −80°C. Viral titer was routinely determined by a 50% tissue culture infectious dose ($TCID_{50}$) assay of HeLa cell monolayer prior to infection.

Reverse transcription-PCR (RT-PCR) and real-time PCR. Total RNA was extracted from heart tissues or culture cells by TRIzol reagent (Invitrogen) and reverse transcripted into cDNA. Subsequently, cDNA was subjected to quantitative real-time PCR using a Lightcycler480 and SYBR green system (TaKaRa) by following the manufacturer's protocol. The primers for real-time PCR were the following: CVB3, 5′-CCC TGA ATG CGG CTA ATC C-3′ (forward) and 5′-AAA CAC GGA CAC CCA AAG TAG TC-3′ (reverse); mouse LC3, 5′-ACA GCA TGG TGA GTG TGT CCA C-3′ (forward) and 5′-ATT GCT GTC CCG AAT GTC TCC-3′ (reverse); mouse TNF-α, 5′-AAG CCT GTA GCC CAC GTC GTA-3′ (forward) and 5′-GGC ACC ACT AGT TGG TTG TCT TTG-3′ (reverse); mouse IL-6, 5′-ACA ACC ACG GCC TTC CCT ACT T-3′ (forward) and 5′-CAC GAT TTC CCA GAG AAC ATG TG-3′ (reverse); mouse ATG5, 5′-TTG ACG TTG GTA ACT GAC AAA GT-3′ (forward) and 5′-TGT GAT GTT CCA AGG AAG AGC-3′ (reverse); mouse glyceraldehyde-3-phosphate dehydrogenase (GAPDH), 5′-CTC TGG AAA GCT GTG GCG TGA TG-3′ (forward) and 5′-ATG CCA GTG AGC TTC CCG TTC AG-3′ (reverse). The expression of individual genes was normalized by GAPDH expression.

CVB3 infection and drug treatment in mice. BALB/c mice in each group were infected by an intraperitoneal injection with 1×10^3 $TCID_{50}$ CVB3 on day 0. To examine the therapeutic effects of suberoylanilide hydroxamic acid (SAHA; Selleck), the solution of SAHA in 2-hydroxypropyl-β-cyclodextrin (HOP-β-CD; Sigma-Aldrich) was prepared as previously described (22). Mice were orally administered daily with 50 mg/kg of body weight of SAHA, starting from the day of virus inoculation. In addition, trichostatin A (TSA; Selleck) was dissolved in dimethyl sulfoxide (DMSO) and injected intraperitoneally into mice at 0.5 mg/kg/day. Ribavirin (Selleck) was dissolved in phosphate-buffered saline (PBS) and injected intraperitoneally into mice at 100 mg/kg/day.

Tissue histopathology. The apical half of the heart was fixed in 4% paraformaldehyde solution, sectioned, and stained with hematoxylin and eosin (H&E). To quantify the number of inflammatory cells in heart tissue, five to 10 fields were randomly selected per section (two sections/per heart, $n = 8$). The average number of inflammatory cells per square millimeter was graphed. The heart sections also were analyzed by terminal deoxynucleotidyl transferase dUTP nick end labeling assay (TUNEL). TUNEL staining was finally developed using diaminobenzidine (DAB). Nuclear staining by hematoxylin was performed as counterstaining. Pictures were acquired with a Nikon Eclipse TE2000-S microscope (Nikon, Tokyo, Japan) with a magnification of ×200 or ×400.

Echocardiography. On day 7 after CVB3 infection, echocardiography was performed on isoflurane-anesthetized mice with a high-resolution ultrasound imaging system (Vevo2100; Visual Sonics) equipped with a 30-MHz microscan transducer. The echocardiographic measurements of left ventricular ejection fraction (LVEF) and left ventricular fractional shortening (LVFS) were performed according to the operator's manual.

Preparation of cardiac myocytes and fibroblasts. Cardiac myocytes from neonatal mice within 72 h of birth were prepared as previously reported (12). Briefly, the hearts were minced finely and subjected to stepwise enzymatic digestion with 0.1% trypsin. The dissociated cells were adsorbed to plastic flasks at 37°C for 2 h for cardiac fibroblast attachment. (i) The nonadherent myocytes were removed, resuspended in complete basal medium, and dispensed into tissue culture wells precoated with collagen protein. After a period of 48 h, the myocytes were attached firmly to the plastic. According to observations on the shape and beating activity of the cells obtained, more than 95% of cells were identified as cardiac myocytes. (ii) The adherent cardiac fibroblasts were washed with PBS and cultured overnight in DMEM supplemented with 10% heat-inactivated fetal bovine serum before use.

Lentiviral particle production and transduction. The short hairpin RNA (shRNA) ATG5 lentiviral plasmids were from Open Biosystems. The recombinant pseudotyped lentivirus was generated by cotransfection of three plasmids, pLKO.1-shATG5/pLKO.1-scramble shRNA, psPAX2, and pMD2.G (Addgene), into 293T cells using Lipofectamine 2000 (Invitrogen). The transduction of cardiac myocytes with lentiviral particle solution expressing either scramble shRNA (Lenti-Ctrl) or ATG5 shRNA (Lenti-shATG5) was described previously (23). Briefly, cells were plated in 24-well plates. On the day of infection, the medium was removed and replaced with viral supernatant to which 8 μg/ml Polybrene had been added. Twenty-four hours after exposure, cells were washed with PBS twice and further incubated for 24 h in fresh culture medium.

Western blotting. For Western blotting, equal amounts of protein were separated by SDS-PAGE and transferred to polyvinylidene difluoride (PVDF) membranes. Membranes were blocked for 1 h with nonfat dry milk solution (5% in Tris-buffered saline) containing 0.1% Tween 20. The blots were probed with primary antibodies for p-p70S6K (catalog number 9208; Cell Signaling Technology), p70S6K (catalog number 9202; Cell Signaling Technology), p-4EBP (catalog number 2855; Cell Signaling Technology), 4EBP (catalog number 9644; Cell Signaling Technology), CAR (catalog number sc-15405; Santa Cruz Biotechnology), LC3 (catalog number L7543; Sigma), Bcl-2 (catalog number 2870; Cell Signaling Technology), and vp1 (catalog number M706401; Dako). Horseradish peroxidase (HRP)-conjugated anti-rabbit (catalog number 7074; Cell Signaling

Technology) or anti-mouse IgG (catalog number 7076; Cell Signaling Technology) was used as a secondary antibody. Immunoreactive bands were visualized by enhanced chemiluminescence (Pierce).

ELISA for proinflammatory cytokines. Levels of TNF-α and IL-6 of cell culture supernatants were determined by enzyme-linked immunosorbent assay (ELISA) (eBioscience) by following the manufacturer's instructions.

Measurement of HDAC activity. HDAC activity was assessed using the HDAC assay kit (Active Motif) according to the manufacturer's instructions. In brief, 10 μg of cardiac myocyte lysate in the presence or absence of 1 μM SAHA was added to each well in 96-well microtiter plates with HDAC substrate, provided by the assay kit, at 37°C for 1 h. The optical density of each well was measured at 405 nm.

Flow cytometric analysis. For flow cytometric analysis, cells were detached from the plate by incubation with 0.25% trypsin. To assess the cell apoptosis, flow cytometric analysis was performed with fluorescein isothiocyanate (FITC)-labeled annexin V and 7-aminoactinomycin D (7-AAD) (eBioscience). Flow cytometric data were acquired on a BD FACSCalibur (BD Biosciences) in CellQuest (BD Biosciences) and analyzed by FlowJo software (Tree Star).

Statistical analysis. All data are shown as the means ± standard errors of the means (SEM). Statistical analysis of the data was performed using the GraphPad Prism (version 5.0) statistical program. The unpaired Student's *t* test was used to compare differences between two groups, whereas comparison of multiple groups was performed using analysis of variance (ANOVA) with *post hoc* tests to compare differences between individual groups. The survival rates of CVB3-infected mice were compared and analyzed with a Kaplan-Meier plot. $P < 0.05$ was considered statistically significant.

RESULTS

Inhibition of HDAC activity exacerbates rather than attenuates CVB3-induced viral myocarditis. To investigate the role of HDAC activity in CVB3-induced viral myocarditis, mice were infected with CVB3 or PBS (control) and then treated daily with SAHA, the first FDA-approved HDACI drug. Contrary to our expectations, in CVB3-infected mice, SAHA treatment resulted in more body weight loss (Fig. 1A) and lower survival rate (Fig. 1B) than those with the non-SAHA-treated group. Histological analysis of heart sections revealed that SAHA treatment led to more focal lesions accompanied by less inflammatory cell infiltration (Fig. 1C and D). In line with the histological result, left ventricular function was deteriorated after SAHA treatment, as revealed by the decreased LVEF and LVFS (Fig. 1E, F, and G). Moreover, SAHA treatment increased serum creatine kinase (CK) and CK-MB levels in those CVB3-infected mice (Fig. 1H and I).

To further confirm that the effect of SAHA was through inhibition of HDAC activity, we treated CVB3-infected mice with a structurally distinct HDAC inhibitor, TSA. We found TSA also resulted in more body weight loss (Fig. 1J) and lower survival rate (Fig. 1K), indicating the exacerbation of viral myocarditis by TSA. Together, those results suggested that inhibition of HDAC activity aggravated rather than attenuated CVB3-induced viral myocarditis.

Exacerbation of viral myocarditis by HDACI is not due to an increased inflammatory response. It is well known that CVB3-induced cardiac injury is caused either by direct virus-induced cellular damage or through inflammatory response (24). Our above-described data showed that the inhibition of HDAC activity reduced inflammatory cell infiltration in the hearts of CVB3-infected mice (Fig. 1C). To confirm the anti-inflammatory effect of HDACI, cardiac myocytes were isolated and exposed to CVB3 in the presence or absence of SAHA for various time periods. As expected, we found SAHA downregulated the expression of proinflammatory cytokines TNF-α and IL-6 at both mRNA (Fig. 2A and B) and protein (Fig. 2C and D) levels. The result was confirmed with another HDAC inhibitor, TSA. We showed that TSA also reduced TNF-α and IL-6 expression both at the mRNA (Fig. 2E and F) and protein (Fig. 2G and H) levels. We have also analyzed the mRNA levels of TNF-α and IL-6 in the heart tissues of CVB3-infected mice. It was found that SAHA significantly downregulated the expression levels of TNF-α (Fig. 2I) and IL-6 (Fig. 2J) *in vivo*.

Those findings further verified the anti-inflammatory properties of HDACIs reported by other investigators (14) and suggested that the exacerbation of viral myocarditis by HDACI treatment was not due to an increased inflammatory response.

HDACI treatment increases CVB3 viral replication. As shown above, HDACI-mediated aggravation of CVB3-induced myocarditis was not due to an increased inflammatory response. Reports also indicate that CVB3 can directly cause the damage to myocytes (24). Thus, we further investigated the effect of HDAC activity on CVB3 viral replication. Our data showed that inhibition of HDAC activity with SAHA increased viral protein vp1 expression (Fig. 3A) and progeny virus production (Fig. 3B) in heart tissues of CVB3-infected mice.

To confirm the role of HDAC activity in CVB3 replication, isolated cardiac myocytes and fibroblasts were infected with CVB3 in the presence or absence of SAHA for various time periods. We showed that SAHA significantly increased CVB3 RNA levels (Fig. 3C and D), protein vp1 expression (Fig. 3E and F), and viral progeny production (Fig. 3G, H, I, and J) in both cardiac myocytes and fibroblasts. Moreover, another HDACI, TSA, also increased CVB3 RNA levels (Fig. 3K), protein vp1 expression (Fig. 3E and F), and viral progeny production (Fig. 3L).

Coxsackie adenovirus receptor (CAR) is the primary receptor for CVB3 to infect permissive cells. It was reported that HDACI increases the expression of CAR in several cancer cell lines (25, 26). To investigate whether HDACI enhanced CVB3 replication by increasing CAR expression and CVB3 entry into cells, cardiac myocytes were treated with SAHA or TSA for various time periods, and CAR expression was determined by Western blotting. We found no significant change in CAR expression in those myocytes after SAHA or TSA treatment (Fig. 3E).

Taken together, these results indicated HDACI treatment significantly increased CVB3 viral replication.

HDACI-increased CVB3 replication is mediated by the enhancement of autophagosome formation. Several reports indicated that autophagosome formation plays a crucial role in CVB3 replication (27, 28). HDACI, including SAHA, have been found to regulate the autophagosome formation by inhibiting mammalian target of rapamycin (mTOR) and upregulating LC3 expression (29). Thus, we further investigated whether HDACI enhanced CVB3 viral replication through regulating the autophagosome formation. Our results showed that SAHA treatment significantly increased the transcript level of LC3 (Fig. 4A), the most widely used marker for autophagosomes, and conversion of LC3-I to LC3-II in CVB3-infected cardiac myocytes (Fig. 4B), indicating the enhanced autophagosome formation by SAHA. Furthermore, in order to examine the mechanism by which SAHA enhanced autophagosome formation, the activity of the mTOR signal path-

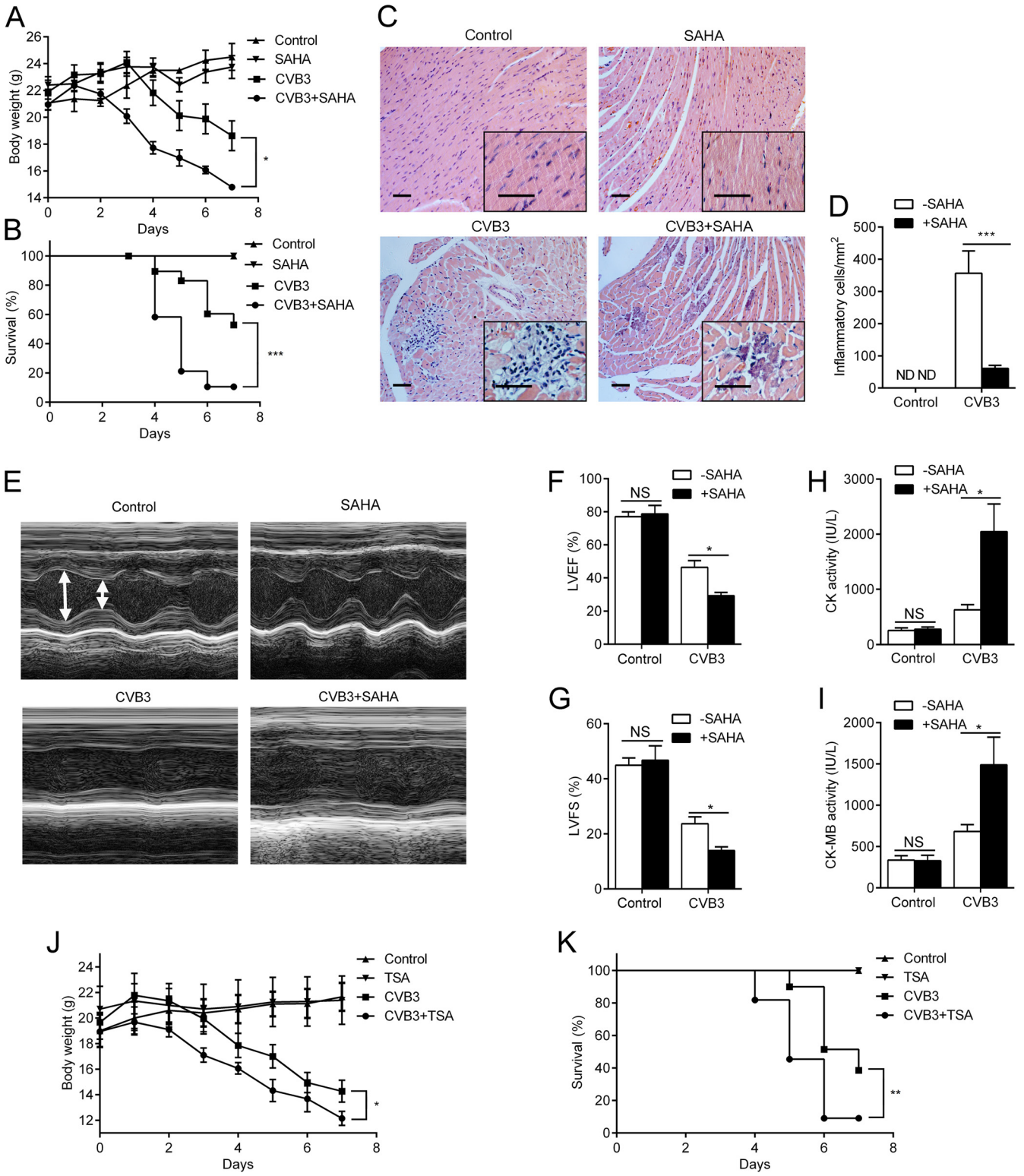

FIG 1 Inhibition of HDAC activity exacerbates rather than attenuates CVB3-induced viral myocarditis. BALB/c mice were sham infected with PBS (control) or infected with CVB3 on day 0 and then treated (or not) with SAHA (50 mg/kg) daily from day 0 to day 7 postinfection (p.i.). The body weight change (A) and survival rate (B) were monitored daily until day 7 p.i. ($n = 26$). (C) Paraffin sections of heart tissues were prepared on day 7 p.i., and cardiac injury was revealed by H&E. (D) The number of inflammatory cells per square millimeter was determined by analysis of the H&E-stained sections ($n = 8$). (E) Representative M-mode echocardiogram recordings on day 7 p.i. Small arrow, systole; large arrow, diastole. LVEF (F) and LVFS (G) from echocardiographic data ($n = 5$) are shown. Serum CK (H) and CK-MB levels (I) were detected on day 7 p.i. ($n = 5$). (J and K) BALB/c mice were sham infected with PBS (control) or infected with CVB3 on day 0 and then treated (or not) with TSA (0.5 mg/kg/day) from day 0 to day 7 p.i. The body weight change (J) and survival rate (K) were monitored daily until day 7 p.i. ($n = 10$). Scale bar, 50 μm. *, $P < 0.05$; **, $P < 0.01$; ***, $P < 0.001$; NS, no significance; ND, not detected.

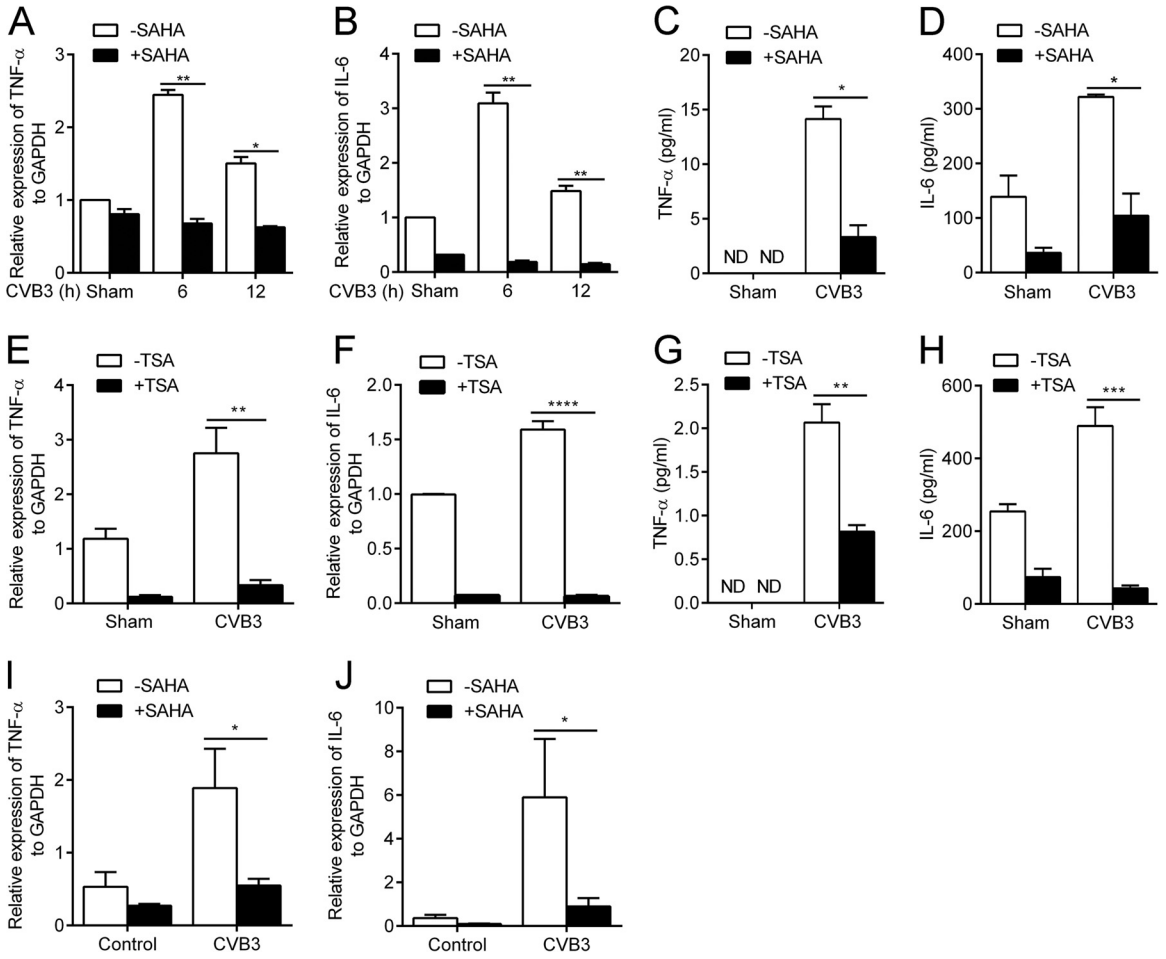

FIG 2 HDACI significantly suppresses CVB3-induced proinflammatory cytokine production. (A and B) Cardiac myocytes were sham infected or infected with CVB3 for the indicated time points at a multiplicity of infection (MOI) of 5 in the presence or absence of 1 μM SAHA. Total RNA was extracted and subjected to real-time RT-PCR for TNF-α (A) and IL-6 (B) transcript level analysis ($n = 3$). (C and D) Cells were treated as described for panels A and B for 24 h. Levels of TNF-α (C) and IL-6 (D) in the cell culture supernatants were determined by ELISA ($n = 3$). (E and F) Cardiac myocytes were sham infected or infected with CVB3 for 12 h (MOI, 5) in the presence or absence of 1 μM TSA. Real-time RT-PCR was used for TNF-α (E) and IL-6 (F) transcript level analysis ($n = 4$). (G and H) Cells were treated as described for panels E and F for 24 h. Levels of TNF-α (G) and IL-6 (H) in the cell culture supernatants were determined by ELISA ($n = 4$). (I and J) BALB/c mice were sham infected with PBS (control) or infected with CVB3 on day 0 and then treated (or not) with SAHA (50 mg/kg) daily from day 0 to day 7 p.i. Total RNA was extracted from heart tissues of the mice on day 7 p.i. and subjected to real-time RT-PCR for TNF-α (I) and IL-6 (J) transcript level analysis ($n = 6$). *, $P < 0.05$; **, $P < 0.01$; ***, $P < 0.001$; ****, $P < 0.0001$; ND, not detected.

way was assessed. The results showed that 4EBP and p70S6K, two substrates of mTOR, were dephosphorylated after SAHA treatment (Fig. 4B), demonstrating the inhibition of the mTOR signal pathway. In agreement with the *in vitro* results, the enhanced autophagy was also observed in CVB-infected mice after SAHA treatment (Fig. 4C). Collectively, these results suggested that SAHA enhanced autophagosome formation in cardiac myocytes, which was through upregulation of LC3 expression and inhibition of the mTOR signal pathway.

To investigate whether SAHA-enhanced autophagosome formation contributed to the increased CVB3 replication, we inhibited myocyte autophagy with wortmannin, a widely used inhibitor of autophagy. Results showed that wortmannin significantly decreased SAHA-enhanced CVB3 viral replication, as demonstrated by the reduced vp1 expression (Fig. 4D) and viral progeny titer (Fig. 4E).

To confirm that the inhibitory effect of wortmannin on CVB3 replication was through the blocking of autophagosome formation rather than through nonspecific effects, we employed an RNA interference approach to further investigate the role of autophagosome formation in SAHA-increased CVB3 replication. Cardiac myocytes were infected with lentivirus expressing shRNA specifically targeting ATG5 (Lenti-shATG5), an autophagy-related protein required for autophagosome formation. Real-time PCR result suggested the efficient knockdown of ATG5 gene transcription in those myocytes (Fig. 4F). Consistent with this, conversion of LC3-I to LC3-II was significantly inhibited after transduction of Lenti-shATG5, indicating the suppression of autophagosome formation (Fig. 4G). In agreement with those results with wortmannin treatment, viral protein expression (Fig. 4G) and supernatant viral titer (Fig. 4H) were significantly decreased by ATG5 knockdown.

Those results demonstrated that HDACI-increased CVB3 replication was mediated by the enhancement of autophagosome formation.

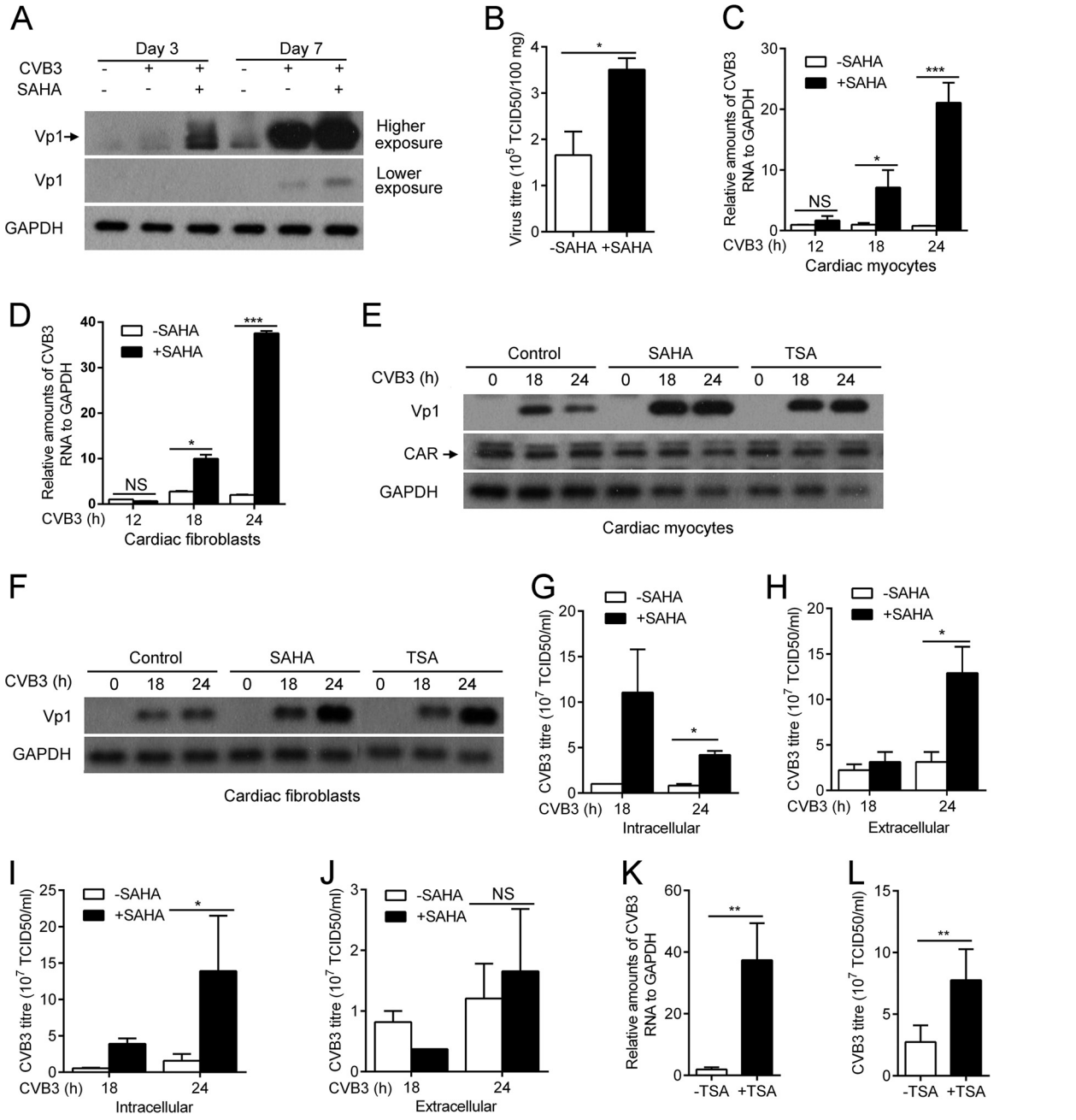

FIG 3 HDACI increases CVB3 viral RNA synthesis, viral protein expression, and viral progeny production. BALB/c mice were sham infected with PBS or infected with CVB3 on day 0 and then either left untreated or treated with SAHA (50 mg/kg) daily from day 0. Hearts were removed aseptically, weighed, and homogenized for Western blotting at the indicated time points (A) and $TCID_{50}$ assay on day 7 p.i. (B) ($n = 6$). GADPH expression was examined as a protein loading control. (C to J) Cardiac myocytes and fibroblasts were infected with CVB3 (MOI, 5) in the presence or absence of 1 μM SAHA for the indicated time points. Viral RNAs of cardiac myocytes (C) and fibroblasts (D) were extracted and determined by real-time RT-PCR ($n = 6$). Cell lysates were collected and immunoblotted with the indicated antibodies for cardiac myocytes (E) and fibroblasts (F). Anti-GAPDH antibody was used as a loading control. Intracellular and extracellular CVB3 titers were measured by $TCID_{50}$ assay for cardiac myocytes (G and H) and fibroblasts (I and J) ($n = 6$). (K and L) Cardiac myocytes were infected with CVB3 (MOI, 5) in the presence or absence of 1 μM TSA for 24 h. Viral RNA was extracted and determined by real-time RT-PCR (K) ($n = 4$), and CVB3 titers in cell culture supernatants were measured by $TCID_{50}$ assay (L) ($n = 4$). *, $P < 0.05$; **, $P < 0.01$; ***, $P < 0.001$; NS, no significance.

Increased CVB3 viral replication by HDACI elevates CVB3-induced myocardial apoptosis. It was reported that the autophagosome supports CVB3 replication. Inhibition of autophagosome formation reduces CVB3 viral replication and CVB3-induced CPE (27). We had shown that HDACI increased CVB3 replication by enhancing autophagosome formation. We further wondered whether HDACI increased CVB3-induced apoptosis. Our results showed that inhibition of HDAC activity with SAHA accumulated acetyl-histone H3 in a dose-dependent manner in cardiac myocytes (Fig. 5A). HDAC activity assay further confirmed the inhi-

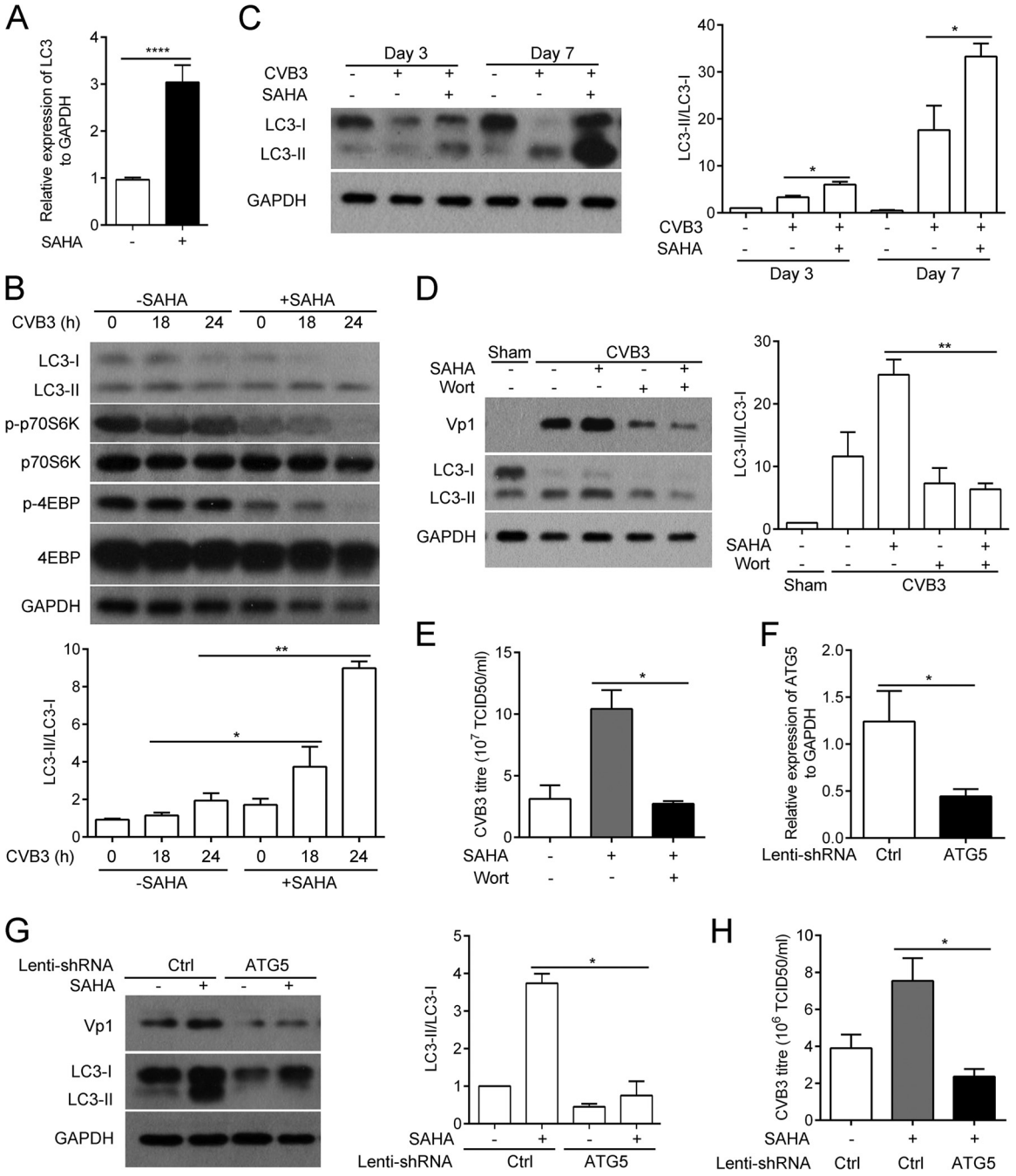

FIG 4 HDACI-increased CVB3 replication is mediated by enhancement of autophagosome formation. (A) Cardiac myocytes were left untreated or were treated with 1 μM SAHA for 18 h, and RNA was extracted from those myocytes and subjected to real-time RT-PCR for LC3 transcript level analysis with GAPDH used as an internal control ($n = 4$). (B) Cardiac myocytes were sham infected or infected with CVB3 in the presence or absence of 1 μM SAHA for the indicated time points. Cell extracts then were analyzed by Western blotting with the indicated antibodies (top), and band intensity of LC3-II and LC3-I was quantified using Image J software (bottom) ($n = 3$). (C) BALB/c mice were left uninoculated or were inoculated with CVB3 and treated with SAHA (50 mg/kg) daily from day 0. Hearts were removed and subjected to Western blotting for LC3 expression analysis on days 3 and 7 p.i. (left), and band intensity of LC3-II and LC3-I was quantified using Image J software (right) ($n = 5$). (D and E) CVB3-infected cardiac myocytes were left untreated or were treated with 1 μM SAHA in the presence or absence of 4 μM wortmannin (wort) for 24 h. (D) Cell extracts were analyzed by Western blotting with the indicated antibodies (left), and the band intensity of LC3-II and LC3-I was quantified using Image J software (right) ($n = 3$). (E) CVB3 titers in cell culture supernatants were determined by $TCID_{50}$ assay ($n = 6$). (F to H) Cardiac myocytes were transduced with lentivirus expressing scramble shRNA (Ctrl) or shRNA targeting ATG5 for 72 h and infected with CVB3 (MOI, 5) in the presence or absence of 1 μM SAHA for another 24 h. (F) Transduction efficiency was quantified by real-time PCR ($n = 4$). (G) Expression of LC3 and vp1 were examined by Western blotting (left), and band intensity of LC3-II and LC3-I was quantified using Image J software (right) ($n = 3$). (H) CVB3 titers in cell culture supernatants were determined by $TCID_{50}$ assay ($n = 3$). *, $P < 0.05$; **, $P < 0.01$; ****, $P < 0.0001$.

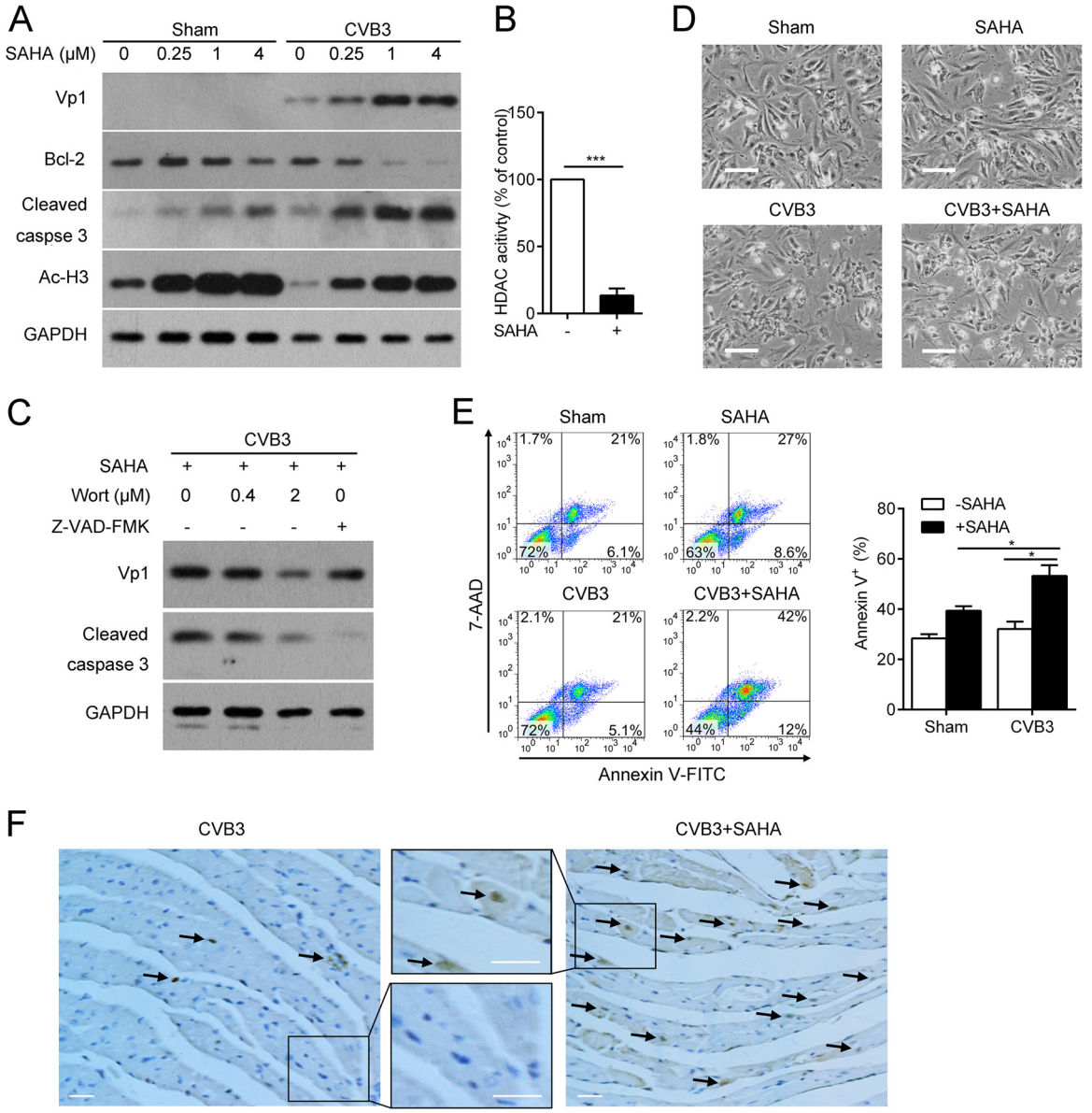

FIG 5 Increased CVB3 viral replication by HDACI elevates CVB3-induced myocardial apoptosis. (A) Cardiac myocytes were sham infected or infected with CVB3 and treated with the indicated concentrations of SAHA for 24 h. Cell extracts were analyzed by Western blotting with the indicated antibodies. (B) The inhibition of HDAC activity with 1 μM SAHA in 10 μg of cardiac myocyte lysate was determined with an HDAC assay kit ($n = 3$). (C) CVB3-infected cardiac myocytes were treated with 1 μM SAHA in the presence or absence of the indicated concentrations of wortmannin (wort) for 24 h. Cell extracts were analyzed by Western blotting with the indicated antibodies. CVB3-infected cardiac myocytes also were treated with 20 μM Z-VAD-FMK for 24 h, which was used as a positive control for cleaved caspase 3 determination. (D and E) Cardiac myocytes were sham infected or infected with CVB3 in the presence or absence of 1 μM SAHA for 24 h. (D) Cell morphology was examined by a light microscope (scale bar, 100 μm). (E) Cells were collected and stained with 7-AAD and FITC-labeled annexin V, followed by flow cytometric analysis. (F) CVB3-infected mice were left untreated or were treated with SAHA (50 mg/kg/day) from day 0 to day 7. On day 7 p.i., cardiac apoptosis in those mice was revealed by TUNEL staining. Brown-stained cells indicated by arrows were TUNEL positive and considered to be apoptotic (scale bar, 25 μm). *, $P < 0.05$; ***, $P < 0.001$.

bition effect of SAHA on HDAC activity (Fig. 5B). SAHA increased CVB3 protein vp1 expression in a dose-dependent manner (Fig. 5A). In parallel with the increased vp1, SAHA markedly decreased antiapoptotic Bcl-2 protein levels and promoted apoptotic effector caspase 3 cleavage (Fig. 5A), suggesting elevated myocardial apoptosis. Conversely, inhibition of CVB3 replication by wortmannin decreased caspase 3 cleavage in a dose-dependent manner (Fig. 5C). Our data also indicated SAHA significantly promoted the CVB3-induced CPE in cardiac myocytes (Fig. 5D). In those CVB3-infected cardiac myocytes, flow cytometric analysis further revealed that the frequency of annexin V-positive (apoptotic) cells was increased by SAHA treatment (Fig. 5E). In agreement with the *in vitro* results, SAHA treatment also increased myocardial apoptosis in hearts of CVB3-infected mice (Fig. 5F).

These findings suggested that the increased CVB3 replication by HDACI resulted in elevated CVB3-induced apoptosis.

Inhibition of viral replication and ensuing myocardial apoptosis ameliorates HDACI-exacerbated viral myocarditis. To fur-

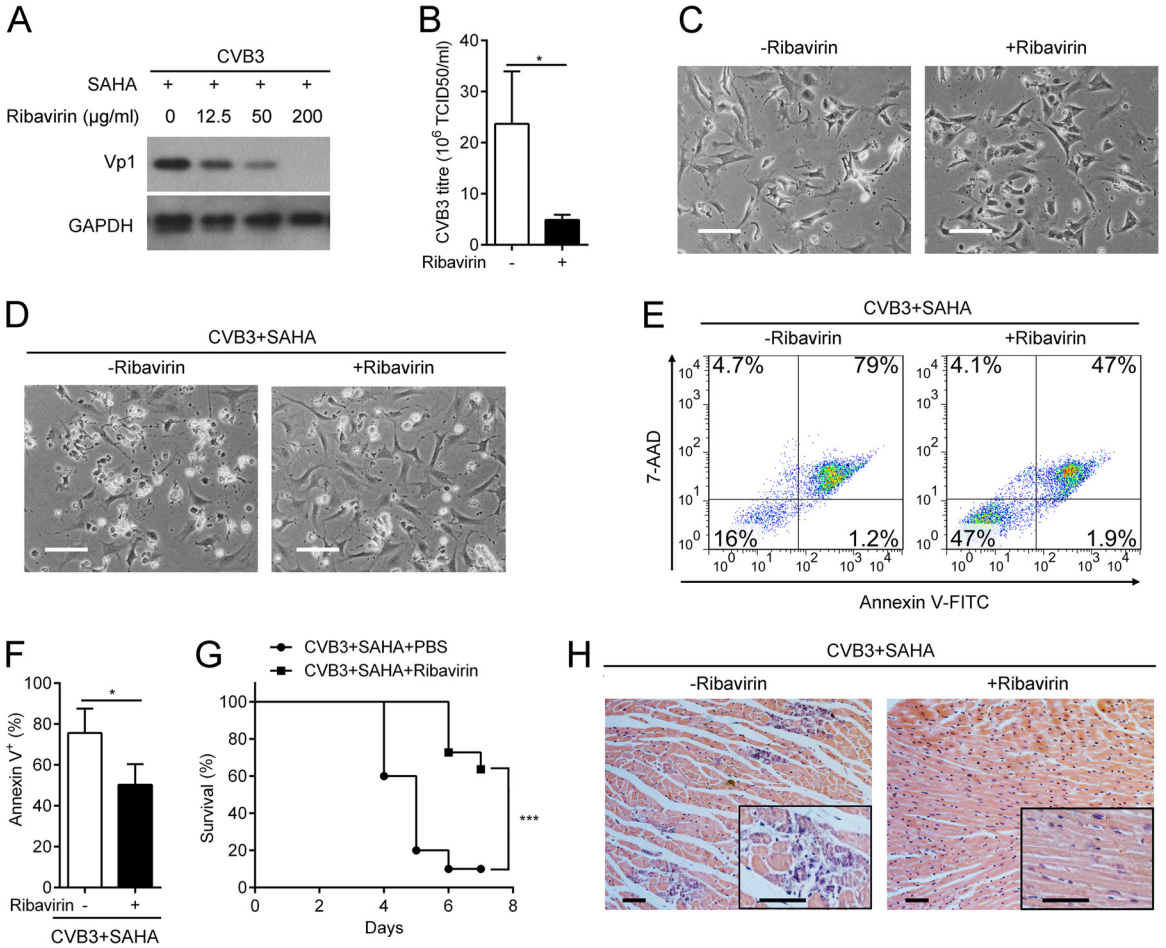

FIG 6 Inhibition of viral replication and ensuing myocardial apoptosis ameliorates HDACI-exacerbated viral myocarditis. (A) CVB3-infected cardiac myocytes (MOI, 5) were treated with 1 μM SAHA and the indicated concentrations of ribavirin for 24 h. Cell extracts were analyzed by Western blotting with the indicated antibodies. (B) CVB3-infected cardiac myocytes (MOI, 5) were treated with 1 μM SAHA and 200 μg/ml ribavirin for 24 h. CVB3 titers in cell culture supernatants were determined by $TCID_{50}$ assay ($n = 4$). (C) Cardiac myocytes were treated with 200 μg/ml ribavirin for 24 h. Cells morphology was examined by light microscope (scale bar, 100 μm). (D to F) CVB3-infected cardiac myocytes (MOI, 5) were treated with 2 μM SAHA in the presence or absence of 800 μg/ml ribavirin for 24 h. (D) Cell morphology was examined by light microscope (scale bar, 100 μm). (E and F) Cells were collected and stained with 7-AAD and FITC-labeled annexin V, followed by flow cytometric analysis ($n = 3$). (G and H) BALB/c mice were infected with CVB3 on day 0 and then simultaneously treated with SAHA (50 mg/kg) and ribavirin (100 mg/kg) or vehicle PBS daily from day 0 to day 7 p.i. (G) Survival rate was monitored daily until day 7 p.i. ($n = 10$). (H) Paraffin sections of heart tissues were prepared on day 7 p.i., and cardiac injury was revealed by H&E (scale bar, 50 μm). *, $P < 0.05$; ***, $P < 0.001$.

ther confirm that HDACI-exacerbated viral myocarditis is due to the increased viral replication and ensuing myocardial apoptosis, we used the antiviral drug ribavirin, a synthetic guanosine analogue (30), to inhibit viral replication in SAHA-treated viral myocarditis mice and monitored parameters of the severity of the disease. We first examined the inhibitory effect of ribavirin on CVB3 viral replication in cardiac myocytes. Consistent with our expectations, ribavirin inhibited both viral protein vp1 expression (Fig. 6A) and progeny virus production (Fig. 6B), whereas it had no CPE on cardiac myocytes (Fig. 6C). Furthermore, ribavirin markedly reduced the CPE of CVB3-infected and SAHA-treated cardiac myocytes (Fig. 6D). Flow cytometric analysis also revealed that ribavirin decreased the frequency of annexin V-positive (apoptotic) cells in those cardiac myocytes (Fig. 6E and F). We next simultaneously treated SAHA-treated viral myocarditis mice with ribavirin. Our results showed that ribavirin significantly improved the survival rate (Fig. 6G) and reversed heart injury (Fig. 6H).

Collectively, these results further confirmed that HDACI was through increasing viral replication and myocardial apoptosis to aggravate viral myocarditis.

DISCUSSION

Excessive inflammatory response evoked by CVB3 infection plays a critical role in the pathogenesis of viral myocarditis. Several approaches have been reported to modulate the inflammatory response for treating viral myocarditis in mouse models (24). Recent studies suggest that inhibition of HDAC activity modulates inflammation response and shows promise in several inflammatory diseases (31). To investigate the role of HDAC activity in viral myocarditis, we treated CVB3-induced myocarditis mice with HDACI. Contrary to our expectation, results showed that HDACI treatment aggravated rather than ameliorated viral myocarditis. Further study suggested that the exacerbation of viral myocarditis was not caused by an increased inflammatory response but by the elevated CVB3 viral replication.

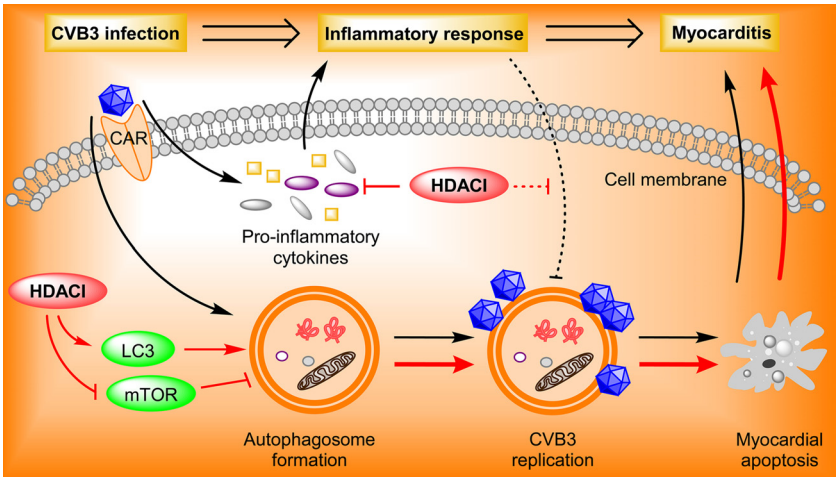

FIG 7 Proposed model of the mechanism of HDACI effect on CVB3-induced myocarditis. CVB3 infection induces both proinflammatory cytokine expression and myocardial autophagosome formation. Proinflammatory cytokines secreted by cardiac myocytes trigger the inflammation response, and the myocardial autophagosome supports CVB3 replication, leading to myocardial apoptosis. Both inflammatory response and myocardial apoptosis are thought to be the major contributors to myocarditis. The HDACI-enhanced autophagosome formation results in excessive CVB3 replication, which aggravates apoptotic myocyte damage and consequent myocarditis. To some extent, inflammation response has a cardioprotective effect by limiting CVB3 replication. Thus, HDACI-mediated inhibition of proinflammatory cytokine expression also might enhance CVB3 replication and contribute to the exacerbation of the disease. The arrow indicates positive regulation, and the crossbar indicates negative regulation. The dotted crossbar represents a likely effect. The well-accepted mechanisms of CVB3-induced myocarditis are colored black, and our proposed mechanisms by which HDACI exacerbates this disease are colored red.

The replication of several viruses has been reported to be modulated by HDAC activity. HDACI activates human immunodeficiency virus (HIV) replication in latently infected cells (32, 33). HDACI increases oncolytic herpes simplex virus (HSV) replication in breast cancer cells (34). Moreover, SAHA is also reported to stimulate hepatitis B virus (HBV) replication (35). On the contrary, hepatitis C virus (HCV) replication is suppressed by SAHA (36). In our study, we found that inhibition of HDAC activity with SAHA or TSA significantly increased CVB3 replication at 24 h postinfection (p.i.) in both cardiac myocytes and fibroblasts. This result is in conflict with the Shim et al. study in which TSA suppressed the CVB3 replication at 24 h p.i. in HeLa cells and protected against CVB3-induced myocardial injury *in vivo* (37). The reason for this apparent discrepancy is unclear. However, we used the CVB3 Nancy strain in the current study, whereas Shim et al. used the Woodruff strain (37). The different CVB3 strain might account for the discrepancy. Of note, we found apoptosis was detected in HeLa cells as early as 8 h after HDACI treatment (data not shown) but not in primary cardiac myocytes as late as 24 h after HDACI treatment (Fig. 5D and E). The result was supported by a prior publication in which proapoptotic activities of HDACI were confined to cancer cells (like HeLa cells), whereas normal cells were less sensitive to HDACI (like primary cardiac myocytes) (38). Those findings demonstrated that it is more appropriate to investigate the role of HDAC activity in CVB3 replication in primary cardiac myocytes rather than in HeLa cells.

Autophagy is a catabolic pathway responsible for maintaining cytoplasmic homeostasis (39, 40). The process involves the formation of vesicles, called autophagosomes, which capture and deliver protein aggregates and damaged organelles to lysosomes for degradation (41, 42). Autophagy also protects against many infections by inducing the lysosome-mediated degradation of invading pathogens. However, previous studies suggest that CVB3 not only evades these protective effects but also exploits autophagy to facilitate its replication (43, 44). The kinase mTOR is a critical regulator of autophagy induction, with activated mTOR suppressing autophagy, whereas the negative regulation of mTOR promotes it (45). Work by other investigators has proved that HDACI activated autophagy by inhibiting mTOR and upregulating LC3 expression in glioblastoma cells (29). Comparable results were observed in cardiac myocytes in the present study. We found SAHA also enhanced autophagosome formation by increasing LC3 expression and inhibiting mTOR activity in cardiac myocytes, which increased CVB3 replication.

It is commonly believed that both direct CVB3-induced myocardial injury and inflammatory response contribute to the development and progression of myocarditis. However, the relative contributions of virus and inflammatory response to myocardial tissue destruction have long been debated (24). In fact, the crucial role of direct CVB3-induced myocardial injury has been supported by numerous studies. For instance, CVB3-infected severe combined immunodeficiency (SCID) mice, which lack mature T and B lymphocyte functions, develop more aggravated myocarditis with increased viral titers (4). Apoptosis is an important mechanism of cardiomyocyte death in viral myocarditis and is associated with the development of fatal heart failure (1, 46). Mitochondrial release of cytochrome *c* is associated with CVB3-induced apoptosis, which triggers the activation of caspases indicated by caspase cleavage (47, 48). In the present study, we found HDACI increased CVB3 replication in cardiac myocytes, which led to decreased antiapoptotic Bcl-2 protein levels and elevated caspase 3 activation in those cells. Consistent with this, HDACI increased CVB3-induced CPE and apoptosis in cardiac myocytes. These results showed that HDACI increased CVB3 viral replication in cardiac myocytes, which promoted myocardial apoptosis.

Although inhibition of HDAC activity has shown promising efficacy in several inflammatory diseases (49), it is more complicated in the virus-induced inflammatory diseases. In addition to

inflammatory responses modulated by HDACI in the progress of these diseases, HDACI also regulates viral replication (such as that of CVB3). CVB3 infection increases both proinflammatory cytokine expression and myocardial autophagosome formation. Autophagosomes support CVB3 viral replication, which leads to myocardial apoptosis (27). Proinflammatory cytokine expression causes inflammation response, which to some extent inhibits CVB3 replication (50). Both inflammation response and apoptosis are thought to be the crucial causes of myocytes damage and ensuing myocarditis (24). In our study, HDACI treatment of CVB3-infected mice aggravated viral myocarditis. The mechanism proposed here was that the HDACI-enhanced autophagosome formation excessively increased viral replication, which dramatically aggravated myocyte damage and consequent myocarditis. Additionally, the HDACI-mediated inhibition of inflammatory response also might contribute to the increased viral replication and the ensuing exacerbation of the disease (Fig. 7). The proposed mechanism was further confirmed by our finding that inhibition of CVB3 viral replication and ensuing myocardial apoptosis by ribavirin significantly reversed HDACI-exacerbated viral myocarditis, as demonstrated by the improvement of survival rate and revision of cardiac injury (whereas there was no improvement in body weight loss; data not shown). In addition, we also assessed the effect of the broad-range caspase inhibitor Z-VAD-FMK on SAHA-treated viral myocarditis mice. We found Z-VAD-FMK did not relieve SAHA-exacerbated viral myocarditis (data not shown), which is supported by Carthy et al., in which Z-VAD-FMK did not inhibit the CVB3-induced CPE in HeLa cells (48).

In conclusion, we report that the inhibition of HDAC activity enhances myocardial autophagosome formation, which leads to elevated CVB3 viral replication and ensuing increased myocardial apoptosis. Viral myocarditis is eventually aggravated rather than ameliorated by HDAC inhibition. We elucidated the role of HDAC activity in viral myocarditis. Moreover, given the importance of HDACI (such as SAHA) in preclinical and clinical treatments for several diseases, possible adverse consequences of administering HDACI should be carefully evaluated in patients infected with viruses, including CVB3.

ACKNOWLEDGMENTS

This work was supported by grants from Major State Basic Research Development Program of China (2013CB530501), the National Natural Science Foundation of China (31470880 and 31470839), The Research Fund for the Doctoral Program of Higher Education of MOE (20133201110013), Jiangsu Provincial Innovative Team, Priority Academic Program Development of Jiangsu Higher Education Institutions (PAPD), and Program for Changjiang Scholars and Innovative Research Team in University (PCSIRT-IRT1075).

We have no conflicting financial interests.

REFERENCES

1. **Esfandiarei M, McManus BM.** 2008. Molecular biology and pathogenesis of viral myocarditis. Annu Rev Pathol **3:**127–155. http://dx.doi.org/10.1146/annurev.pathmechdis.3.121806.151534.
2. **Tam PE.** 2006. Coxsackievirus myocarditis: interplay between virus and host in the pathogenesis of heart disease. Viral Immunol **19:**133–146. http://dx.doi.org/10.1089/vim.2006.19.133.
3. **Van Linthout S, Savvatis K, Miteva K, Peng J, Ringe J, Warstat K, Schmidt-Lucke C, Sittinger M, Schultheiss HP, Tschope C.** 2011. Mesenchymal stem cells improve murine acute coxsackievirus B3-induced myocarditis. Eur Heart J **32:**2168–2178. http://dx.doi.org/10.1093/eurheartj/ehq467.
4. **Chow LH, Beisel KW, McManus BM.** 1992. Enteroviral infection of mice with severe combined immunodeficiency. Evidence for direct viral pathogenesis of myocardial injury. Lab Investig **66:**24–31.
5. **Yuan JP, Zhao W, Wang HT, Wu KY, Li T, Guo XK, Tong SQ.** 2003. Coxsackievirus B3-induced apoptosis and caspase-3. Cell Res **13:**203–209. http://dx.doi.org/10.1038/sj.cr.7290165.
6. **Mason JW, O'Connell JB, Herskowitz A, Rose NR, McManus BM, Billingham ME, Moon TE.** 1995. A clinical trial of immunosuppressive therapy for myocarditis. The Myocarditis Treatment Trial Investigators. N Engl J Med **333:**269–275. http://dx.doi.org/10.1056/nejm199508033330501.
7. **Matsumori A, Yamada T, Suzuki H, Matoba Y, Sasayama S.** 1994. Increased circulating cytokines in patients with myocarditis and cardiomyopathy. Br Heart J **72:**561–566.
8. **Levine B, Kalman J, Mayer L, Fillit HM, Packer M.** 1990. Elevated circulating levels of tumor necrosis factor in severe chronic heart failure. N Engl J Med **323:**236–241. http://dx.doi.org/10.1056/nejm199007263230405.
9. **Yue Y, Gui J, Xu W, Xiong S.** 2011. Gene therapy with CCL2 (MCP-1) mutant protects CVB3-induced myocarditis by compromising Th1 polarization. Mol Immunol **48:**706–713. http://dx.doi.org/10.1016/j.molimm.2010.11.018.
10. **Yue Y, Gui J, Ai W, Xu W, Xiong S.** 2011. Direct gene transfer with IP-10 mutant ameliorates mouse CVB3-induced myocarditis by blunting Th1 immune responses. PLoS One **6:**e18186. http://dx.doi.org/10.1371/journal.pone.0018186.
11. **Lv K, Xu W, Wang C, Niki T, Hirashima M, Xiong S.** 2011. Galectin-9 administration ameliorates CVB3 induced myocarditis by promoting the proliferation of regulatory T cells and alternatively activated Th2 cells. Clin Immunol **140:**92–101. http://dx.doi.org/10.1016/j.clim.2011.03.017.
12. **Gui J, Yue Y, Chen R, Xu W, Xiong S.** 2012. A20 (TNFAIP3) alleviates CVB3-induced myocarditis via inhibiting NF-kappaB signaling. PLoS One **7:**e46515. http://dx.doi.org/10.1371/journal.pone.0046515.
13. **Wang Y, Gao B, Xiong S.** 2014. Involvement of NLRP3 inflammasome in CVB3-induced viral myocarditis. Am J Physiol Heart Circ Physiol **307:**H1438–1447. http://dx.doi.org/10.1152/ajpheart.00441.2014.
14. **Wang L, de Zoeten EF, Greene MI, Hancock WW.** 2009. Immunomodulatory effects of deacetylase inhibitors: therapeutic targeting of FOXP3+ regulatory T cells. Nat Rev Drug Discov **8:**969–981. http://dx.doi.org/10.1038/nrd3031.
15. **Shakespear MR, Halili MA, Irvine KM, Fairlie DP, Sweet MJ.** 2011. Histone deacetylases as regulators of inflammation and immunity. Trends Immunol **32:**335–343. http://dx.doi.org/10.1016/j.it.2011.04.001.
16. **Gao B, Wang Y, Xu W, Li S, Li Q, Xiong S.** 2013. Inhibition of histone deacetylase activity suppresses IFN-gamma induction of tripartite motif 22 via CHIP-mediated proteasomal degradation of IRF-1. J Immunol **191:**464–471. http://dx.doi.org/10.4049/jimmunol.1203533.
17. **Lin HS, Hu CY, Chan HY, Liew YY, Huang HP, Lepescheux L, Bastianelli E, Baron R, Rawadi G, Clement-Lacroix P.** 2007. Anti-rheumatic activities of histone deacetylase (HDAC) inhibitors in vivo in collagen-induced arthritis in rodents. Br J Pharmacol **150:**862–872. http://dx.doi.org/10.1038/sj.bjp.0707165.
18. **Glauben R, Batra A, Fedke I, Zeitz M, Lehr HA, Leoni F, Mascagni P, Fantuzzi G, Dinarello CA, Siegmund B.** 2006. Histone hyperacetylation is associated with amelioration of experimental colitis in mice. J Immunol **176:**5015–5022.
19. **Tao R, de Zoeten EF, Ozkaynak E, Chen C, Wang L, Porrett PM, Li B, Turka LA, Olson EN, Greene MI, Wells AD, Hancock WW.** 2007. Deacetylase inhibition promotes the generation and function of regulatory T cells. Nat Med **13:**1299–1307. http://dx.doi.org/10.1038/nm1652.
20. **Mishra N, Reilly CM, Brown DR, Ruiz P, Gilkeson GS.** 2003. Histone deacetylase inhibitors modulate renal disease in the MRL-lpr/lpr mouse. J Clin Investig **111:**539–552. http://dx.doi.org/10.1172/jci16153.
21. **Finkelstein RA, Li Y, Liu B, Shuja F, Fukudome E, Velmahos GC, deMoya M, Alam HB.** 2010. Treatment with histone deacetylase inhibitor attenuates MAP kinase mediated liver injury in a lethal model of septic shock. J Surg Res **163:**146–154. http://dx.doi.org/10.1016/j.jss.2010.04.024.
22. **Hrzenjak A, Moinfar F, Kremser ML, Strohmeier B, Petru E, Zatloukal K, Denk H.** 2010. Histone deacetylase inhibitor vorinostat suppresses the growth of uterine sarcomas in vitro and in vivo. Mol Cancer **9:**49. http://dx.doi.org/10.1186/1476-4598-9-49.
23. **Bonci D, Cittadini A, Latronico MV, Borello U, Aycock JK, Drusco A, Innocenzi A, Follenzi A, Lavitrano M, Monti MG, Ross J, Jr, Naldini L, Peschle C, Cossu G, Condorelli G.** 2003. "Advanced"

generation lentiviruses as efficient vectors for cardiomyocyte gene transduction in vitro and in vivo. Gene Ther **10:**630–636. http://dx.doi.org/10.1038/sj.gt.3301936.
24. **Corsten MF, Schroen B, Heymans S.** 2012. Inflammation in viral myocarditis: friend or foe? Trends Mol Med **18:**426–437. http://dx.doi.org/10.1016/j.molmed.2012.05.005.
25. **Kim DR, Park MY, Lim HJ, Park JS, Cho YJ, Lee SW, Yoon HI, Lee JH, Kim YS, Lee CT.** 2012. Combination therapy of conditionally replicating adenovirus and histone deacetylase inhibitors. Int J Mol Med **29:**218–224. http://dx.doi.org/10.3892/ijmm.2011.831.
26. **Sachs MD, Ramamurthy M, Poel H, Wickham TJ, Lamfers M, Gerritsen W, Chowdhury W, Li Y, Schoenberg MP, Rodriguez R.** 2004. Histone deacetylase inhibitors upregulate expression of the coxsackie adenovirus receptor (CAR) preferentially in bladder cancer cells. Cancer Gene Ther **11:**477–486. http://dx.doi.org/10.1038/sj.cgt.7700726.
27. **Wong J, Zhang J, Si X, Gao G, Mao I, McManus BM, Luo H.** 2008. Autophagosome supports coxsackievirus B3 replication in host cells. J Virol **82:**9143–9153. http://dx.doi.org/10.1128/jvi.00641-08.
28. **Alirezaei M, Flynn CT, Whitton JL.** 2012. Interactions between enteroviruses and autophagy in vivo. Autophagy **8:**973–975. http://dx.doi.org/10.4161/auto.20160.
29. **Gammoh N, Lam D, Puente C, Ganley I, Marks PA, Jiang X.** 2012. Role of autophagy in histone deacetylase inhibitor-induced apoptotic and nonapoptotic cell death. Proc Natl Acad Sci U S A **109:**6561–6565. http://dx.doi.org/10.1073/pnas.1204429109.
30. **Patterson JL, Fernandez-Larsson R.** 1990. Molecular mechanisms of action of ribavirin. Rev Infect Dis **12:**1139–1146.
31. **Fairlie DP, Sweet MJ.** 2012. HDACs and their inhibitors in immunology: teaching anticancer drugs new tricks. Immunol Cell Biol **90:**3–5. http://dx.doi.org/10.1038/icb.2011.105.
32. **Contreras X, Schweneker M, Chen CS, McCune JM, Deeks SG, Martin J, Peterlin BM.** 2009. Suberoylanilide hydroxamic acid reactivates HIV from latently infected cells. J Biol Chem **284:**6782–6789. http://dx.doi.org/10.1074/jbc.M807898200.
33. **Shirakawa K, Chavez L, Hakre S, Calvanese V, Verdin E.** 2013. Reactivation of latent HIV by histone deacetylase inhibitors. Trends Microbiol **21:**277–285. http://dx.doi.org/10.1016/j.tim.2013.02.005.
34. **Cody JJ, Markert JM, Hurst DR.** 2014. Histone deacetylase inhibitors improve the replication of oncolytic herpes simplex virus in breast cancer cells. PLoS One **9:**e92919. http://dx.doi.org/10.1371/journal.pone.0092919.
35. **Wang YC, Yang X, Xing LH, Kong WZ.** 2013. Effects of SAHA on proliferation and apoptosis of hepatocellular carcinoma cells and hepatitis B virus replication. World J Gastroenterol **19:**5159–5164. http://dx.doi.org/10.3748/wjg.v19.i31.5159.
36. **Sato A, Saito Y, Sugiyama K, Sakasegawa N, Muramatsu T, Fukuda S, Yoneya M, Kimura M, Ebinuma H, Hibi T, Ikeda M, Kato N, Saito H.** 2013. Suppressive effect of the histone deacetylase inhibitor suberoylanilide hydroxamic acid (SAHA) on hepatitis C virus replication. J Cell Biochem **114:**1987–1996. http://dx.doi.org/10.1002/jcb.24541.
37. **Shim SH, Park JH, Ye MB, Nam JH.** 2013. Histone deacetylase inhibitors suppress coxsackievirus B3 growth in vitro and myocarditis induced in mice. Acta Virol **57:**462–466. http://dx.doi.org/10.4149/av_2013_04_462.
38. **Marks P, Rifkind RA, Richon VM, Breslow R, Miller T, Kelly WK.** 2001. Histone deacetylases and cancer: causes and therapies. Nat Rev Cancer **1:**194–202. http://dx.doi.org/10.1038/35106079.
39. **Senft D, Ronai ZA.** 2015. UPR, autophagy, and mitochondria crosstalk underlies the ER stress response. Trends Biochem Sci **40:**141–148. http://dx.doi.org/10.1016/j.tibs.2015.01.002.
40. **Levine B, Packer M, Codogno P.** 2015. Development of autophagy inducers in clinical medicine. J Clin Investig **125:**14–24. http://dx.doi.org/10.1172/jci73938.
41. **Kuma A, Mizushima N.** 2010. Physiological role of autophagy as an intracellular recycling system: with an emphasis on nutrient metabolism. Semin Cell Dev Biol **21:**683–690. http://dx.doi.org/10.1016/j.semcdb.2010.03.002.
42. **Hamai A, Codogno P.** 2012. New targets for acetylation in autophagy. Sci Signal **5:**pe29. http://dx.doi.org/10.1126/scisignal.2003187.
43. **Kemball CC, Alirezaei M, Flynn CT, Wood MR, Harkins S, Kiosses WB, Whitton JL.** 2010. Coxsackievirus infection induces autophagy-like vesicles and megaphagosomes in pancreatic acinar cells in vivo. J Virol **84:**12110–12124. http://dx.doi.org/10.1128/jvi.01417-10.
44. **Alirezaei M, Flynn CT, Wood MR, Whitton JL.** 2012. Pancreatic acinar cell-specific autophagy disruption reduces coxsackievirus replication and pathogenesis in vivo. Cell Host Microbe **11:**298–305. http://dx.doi.org/10.1016/j.chom.2012.01.014.
45. **Weidberg H, Shvets E, Elazar Z.** 2011. Biogenesis and cargo selectivity of autophagosomes. Annu Rev Biochem **80:**125–156. http://dx.doi.org/10.1146/annurev-biochem-052709-094552.
46. **Kyto V, Saraste A, Saukko P, Henn V, Pulkki K, Vuorinen T, Voipio-Pulkki LM.** 2004. Apoptotic cardiomyocyte death in fatal myocarditis. Am J Cardiol **94:**746–750. http://dx.doi.org/10.1016/j.amjcard.2004.05.056.
47. **Carthy CM, Yanagawa B, Luo H, Granville DJ, Yang D, Cheung P, Cheung C, Esfandiarei M, Rudin CM, Thompson CB, Hunt DW, McManus BM.** 2003. Bcl-2 and Bcl-xL overexpression inhibits cytochrome c release, activation of multiple caspases, and virus release following coxsackievirus B3 infection. Virology **313:**147–157. http://dx.doi.org/10.1016/S0042-6822(03)00242-3.
48. **Carthy CM, Granville DJ, Watson KA, Anderson DR, Wilson JE, Yang D, Hunt DW, McManus BM.** 1998. Caspase activation and specific cleavage of substrates after coxsackievirus B3-induced cytopathic effect in HeLa cells. J Virol **72:**7669–7675.
49. **Bush EW, McKinsey TA.** 2010. Protein acetylation in the cardiorenal axis: the promise of histone deacetylase inhibitors. Circ Res **106:**272–284. http://dx.doi.org/10.1161/circresaha.109.209338.
50. **Wada H, Saito K, Kanda T, Kobayashi I, Fujii H, Fujigaki S, Maekawa N, Takatsu H, Fujiwara H, Sekikawa K, Seishima M.** 2001. Tumor necrosis factor-alpha (TNF-alpha) plays a protective role in acute viralmyocarditis in mice: a study using mice lacking TNF-alpha. Circulation **103:**743–749. http://dx.doi.org/10.1161/01.CIR.103.5.743.